

Improved Encoding for Overfitted Video Codecs

Thomas Leguay^{†*}, Théo Ladune[†], Pierrick Philippe[†], Olivier Déforges^{*}

[†]Orange Innovation, France, firstname.lastname@orange.com

^{*}Univ Rennes, INSA Rennes, CNRS, IETR (UMR 6164), France, firstname.lastname@insa-rennes.fr

Abstract—Overfitted neural video codecs offer a decoding complexity orders of magnitude smaller than their autoencoder counterparts. Yet, this low complexity comes at the cost of limited compression efficiency, in part due to their difficulty capturing accurate motion information. This paper proposes to guide motion information learning with an optical flow estimator. A joint rate-distortion optimization is also introduced to improve rate distribution across the different frames. These contributions maintain a low decoding complexity of 1300 multiplications per pixel while offering compression performance close to the conventional codec HEVC and outperforming other overfitted codecs. This work is made open-source at <https://orange-opensource.github.io/Cool-Chic/>.

Index Terms—Neural video coding, low complexity, overfitting

I. INTRODUCTION & RELATED WORKS

Video compression is dominated by the conventional codecs H.264/AVC, H.265/HEVC and H.266/VVC [1]–[3]. One of their main principles is to optimize the video RD (rate-distortion) cost during encoding to find the best decoder parameters. Successive generations of codecs offer additional decoding options, increasing compression performance while maintaining low decoder complexity.

Recently, autoencoder-based codecs [4]–[7] have leveraged neural networks to automatically design (learn) a codec and now challenge the state-of-the-art conventional codec VVC. They do not rely on encoding-time RD optimization of the decoder parameters. This is delegated to an offline training stage where all the parameters are learned and set once and for all. Consequently, their decoder must provision parameters to deal with all possible signals resulting in an important complexity, up to a million multiplications per decoded pixel [4], [5]. This makes their practical use less attractive, as they are expected to run on a variety of low-power devices.

Overfitting-based codecs [8]–[13] bridge the gap between these two paradigms by introducing encoding-time RD optimization into a learned codec. To this end, a decoder is learned for each image or video. The successive refinements of the overfitted image codec Cool-chic [8]–[11] demonstrate that a neural decoder with 2000 multiplications per decoded pixel is competitive with VVC for image coding.

Several works extend Cool-chic to video coding [11], [14]. Although these methods guarantee low-complexity decoding, they are far from challenging conventional methods in terms of rate-distortion performance. These approaches differ in their exploitation of temporal redundancies. C3 [11] extends the spatial entropy module to also account for temporal redundancies. Cool-chic video [14] relies on residual coding and motion

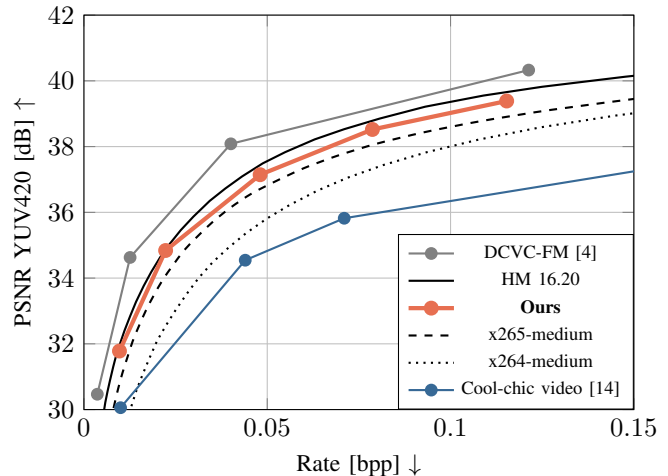


Fig. 1: Random access rate-distortion graphs. HEVC class B. PSNR computed in YUV420 domain.

TABLE I: BD-rates vs. HEVC (HM 16.20) on the 9 first frames of the HEVC sequences. Distortion in YUV420.

| | Random access BD-rate vs. HM 16.20 [%] ↓ | | | |
|----------------------|--|-------------|-------------|------------|
| | Class B | Class C | Class E | Average |
| Ours | 4.6 | 12.4 | 10.8 | 9.3 |
| x265-medium | 30.4 | 31.5 | 46.7 | 36.2 |
| x264-medium | 85.7 | 48.6 | 83.2 | 72.5 |
| Cool-chic video [14] | 118.8 | 100.3 | 105.2 | 108.1 |

compensation to leverage temporal redundancies. Yet, Cool-chic video struggles to capture challenging motion leading to degraded temporal prediction and limiting its compression performance.

This work improves Cool-chic video [14] by guiding the motion information learning with a pre-trained optical flow estimator, ensuring high-quality motion data while maintaining low decoder complexity. An additional joint optimization stage is introduced to better allocate the rate across frames. These contributions result in a lightweight video codec (1300 multiplications per decoded pixel) approaching HEVC compression performance and outperforming other overfitted codecs.

II. PROPOSED DECODING SCHEME

Figure 2 illustrates the proposed decoding scheme for a $H \times W$ frame \hat{x}_t with two references (\hat{x}_{ref_1} , \hat{x}_{ref_2}). Each frame is decoded with their own pair of Cool-chic decoders [8]: one for the motion and the other for the residue. A Cool-chic decoder is made of 3 NNs (neural networks) and reconstructs data from

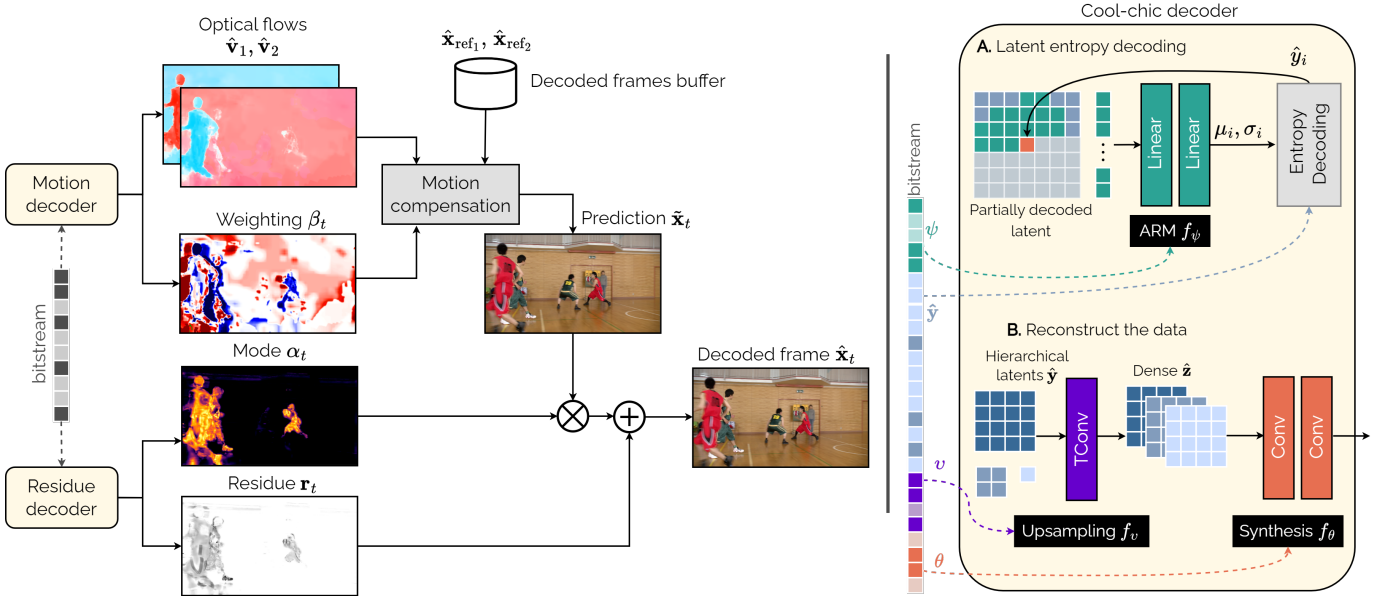


Fig. 2: Decoding pipeline of an inter frame with two references. Cool-chic decoder diagram is from Blard *et al.* [10].

a latent representation in two steps. *i*) the auto-regressive NN f_ψ drives an entropy decoder to obtain a hierarchical latent representation \hat{y}_t from the bitstream. *ii*) the upsampling NN f_v converts the hierarchical latents into a dense representation, fed to the synthesis NN f_θ to obtain the decoded data.

The motion decoder outputs two optical flows \hat{v}_1, \hat{v}_2 and a bi-directional prediction weighting $\beta_t \in [0, 1]^{H \times W}$. The flows are pixel-wise motion fields indicating each pixel displacement between the frame and its references. They are used to obtain a temporal prediction \tilde{x}_t via a weighted bilinear warping:

$$\tilde{x}_t = \beta_t \text{warp}(\hat{x}_{\text{ref}_1}, \hat{v}_1) + (1 - \beta_t) \text{warp}(\hat{x}_{\text{ref}_2}, \hat{v}_2). \quad (1)$$

The residue decoder outputs a coding mode $\alpha_t \in [0, 1]^{H \times W}$ and a residue r_t . The coding mode is a pixel-wise continuous weighting masking out the prediction if it is counterproductive. The residue conveys the non-predicted information. It is added to the masked prediction to obtain the decoded frame \hat{x}_t :

$$\hat{x}_t = \alpha_t \tilde{x}_t + r_t. \quad (2)$$

A fixed downsampling (*e.g.* bilinear) of the decoded frame is used to obtain a frame in the YUV420 domain. The proposed decoding process also considers frames with 1 reference (P-frame) and no reference (I-frame). For P-frames, only a single optical flow is used and $\beta_t = 1$. I-frames are entirely conveyed via the residue r_t *i.e.* $\alpha_t = 0$.

The key difference with prior works is the two separated Cool-chic decoders for each frame. Prior methods have a unique Cool-chic decoder for each frame [14] or shared between several frames [11].

III. ENCODING METHOD

A. Joint optimization of successive frames

Videos are encoded by overfitting the decoder parameters and the latent representation of each frame to minimize the

video RD cost. One key issue to obtain competitive performance is to properly allocate the rate between the different video frames. For instance, in the 9-frame hierarchical structure presented in Fig. 3, the I-frame and the middle B-frame are used as reference for 4 frames whereas some other B-frames never serve as reference. Consequently, it is usually more effective to allocate more rate to the frames often used as reference. If such frames exhibit less distortion, then the subsequent predictions also present less distortion allowing for a lower overall rate-distortion cost.

Previous work [14] performs frame-wise rate allocation using a different rate constraint λ_t for each frame, coupled with frame-wise RD optimisation. With this method, each frame is encoded separately according to its own RD cost:

$$\mathcal{L}_t = D(x_t, \hat{x}_t) + \lambda_t (R(\hat{y}_t^m) + R(\hat{y}_t^r)), \quad (3)$$

where \hat{y}_t^m and \hat{y}_t^r are the latent representations respectively carrying the motion and the residue information. Yet, determining the proper λ_t is a difficult issue as it varies with the video movements, spatial complexity and bitrate.

To solve this issue, we propose an additional training step which complements the frame-wise RD optimization. It refines

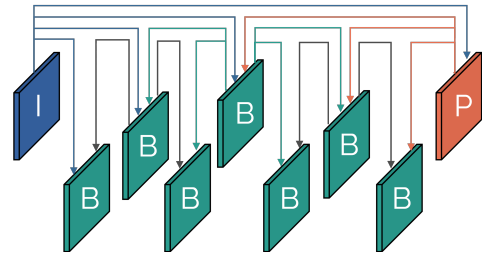


Fig. 3: Random access coding configuration.

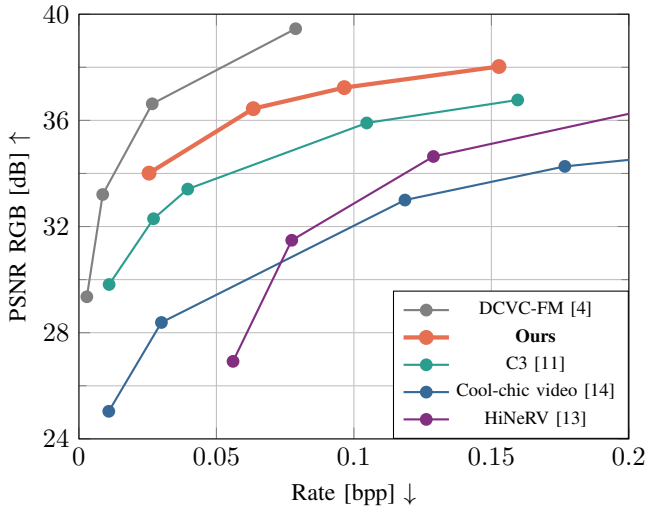


Fig. 4: Random access rate-distortion graphs. UVG dataset. PSNR in RGB domain.

all the parameters (latent representation and neural networks) of all frames to minimize the overall video RD-cost:

$$\mathcal{L} = \sum_t D(\mathbf{x}_t, \hat{\mathbf{x}}_t) + \lambda \sum_t R(\hat{\mathbf{y}}_t^m) + R(\hat{\mathbf{y}}_t^r). \quad (4)$$

This permits to have a single rate constraint λ balancing the total distortion of the video against the total rate. Within this overall bit budget, the optimization process automatically allocates the rate across video frames.

B. Learning more accurate motion information

Having a dedicated motion decoder allows to pre-train only the motion-related parameters of the system and prevents interfering with the parameters dedicated to the residue. We introduce a pre-training stage to first learn accurate motion information. Then, the residue is learned without undoing the motion representation since it has its own representation.

Estimating accurate motions is a challenging task involving elaborate strategies [15]. Modern approaches [16]–[18] rely on 4D correlation volumes, hierarchical refinements and ground truth motions from annotated datasets. Such pre-trained optical flow estimators are leveraged by state-of-the-art autoencoders for video coding [4]–[6] to obtain accurate motion information subsequently compressed and sent to the decoder. However, none of overfitted codecs [11], [13], [14], [19] exploit these optical flow estimators.

Inspired by autoencoders, we capitalize on existing optical flow estimators by pre-training the motion decoder to replicate motions estimated by RAFT [16]. The optical flows estimated by RAFT between a frame \mathbf{x}_t and its references are denoted \mathbf{v}_1 and \mathbf{v}_2 . The encoding of \mathbf{x}_t starts by training only the motion decoder to represent the RAFT-estimated flows. This is achieved by minimizing:

$$\mathcal{L} = D(\mathbf{v}_1, \hat{\mathbf{v}}_1) + D(\mathbf{v}_2, \hat{\mathbf{v}}_2) + \lambda_v (R(\hat{\mathbf{v}}_1) + R(\hat{\mathbf{v}}_2)), \quad (5)$$

TABLE II: Decoder architectures. Layers are denoted with k - i - o for kernel size (if any), input and output features. TConv is a transposed convolution with a stride of 2. Motion synthesis outputs either $m = 2$ (P-frame) or $m = 5$ (B-frame) features.

| Decoder | ARM f_ψ | Upsampling f_ν | Synthesis f_θ | Complexity [MAC/pixel] |
|---------|---|--------------------|--|--------------------------|
| Intra | Linear 24-24 Linear 24-24 Linear 24-2 | TConv 8-1-1 | Conv 1-7-40 Conv 1-40-3 Conv 3-3-3 Conv 3-3-3 | 2292 |
| Residue | Linear 8-8 Linear 8-8 Linear 8-2 | TConv 8-1-1 | Conv 1-7-28 Conv 1-28-4 Conv 3-4-4 | 774 |
| Motion | Linear 8-8 Linear 8-2 | TConv 8-1-1 | Conv 1-7-9 Conv 1-9- m Conv 3- m - m | 257 (P) or 473 (B) |

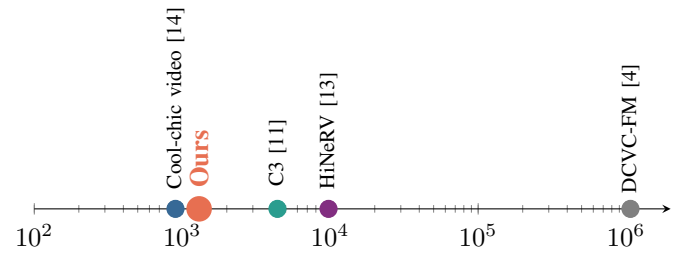


Fig. 5: Decoding complexity (MAC per decoded pixel)

where $\hat{\mathbf{v}}$ denotes the compressed version of the optical flows, D a distortion metric, R the rate and λ_v a rate constraint. The optical flow estimator is only used at the encoder as a guidance, maintaining a low-complexity decoder. This frame-wise pre-training learns accurate motions while taking their rate into account.

IV. EXPERIMENTS

A. Rate-distortion performance

The proposed method is evaluated on the HEVC and UVG datasets [20], [21] against a wide variety of other codecs: conventional codecs such as AVC (x264-medium) and HEVC (x265-medium, HM), overfitted codecs with Cool-chic video [14], C3 [11] and HiNeRV [13] and the autoencoder DCVC-FM [4]. To ensure fair comparison, conventional codecs are evaluated in the YUV420 domain on the HEVC test sequences while overfitted codecs and autoencoders are evaluated in the RGB domain on the UVG sequences. Experiments are carried out on the first 9 frames of each video, with the random access coding configuration (Fig. 3). BD-rate [22] (relative rate for identical quality) is used to quantify gap performance between codecs.

Table II presents the architecture of the intra, motion and residue decoders. Encoding starts with a frame-wise pre-training of the motion information for 10^4 iterations. This is followed by a joint optimization of the rate-distortion cost for 10^5 iterations. Both stages schedule learning rate, noise and softround parameters similarly to C3 [11]. The following rate constraint λ values are used :

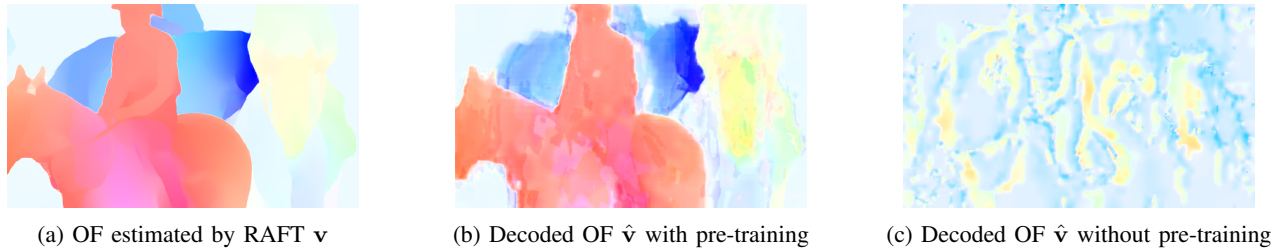


Fig. 6: Importance of the optical flow (OF) pre-training for the *RaceHorses* sequence (HEVC C).

$\{0.05, 0.01, 0.0025, 0.001, 0.0005\}$. It is also found empirically that setting $\lambda_v = 20\lambda$ for the motion pre-training leads to better results.

Figures 1 and 4 present the rate-distortion curves obtained by the proposed method. It significantly outperforms other overfitted codecs (C3, Cool-chic and HiNeRV). Even in the more challenging YUV420 domain, we achieve better compression performance than x264-medium and x265-medium and come close to the HM. Table I shows the BD-rate, highlighting the improvement offered by the proposed system against Cool-chic video. This is particularly interesting since the main difference between these two systems is the encoding enhancement offered by this work.

Beside its compelling compression performance, the proposed system also features a lightweight decoder. Table II details its complexity and Fig. 5 compares it to other overfitted and autoencoder-based codecs. The proposed system maintains the low-complexity of Cool-chic video and C3. It is less complex than NeRV-based codecs *e.g.* HiNeRV and than autoencoder-based codecs such as DCVC-DC.

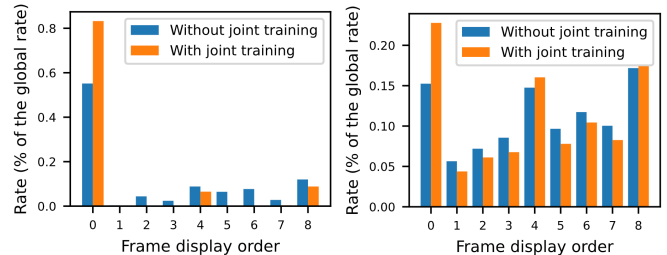
B. Ablation

Table III presents the impact of removing each contribution individually. Removing the motion decoder pre-training significantly degrades classes B and C, but proves neutral for class E. This is due to class E sequences having smaller movements. For sequences with substantial movements, this pre-training enhances optical flows accuracy, as in Fig 6.

Joint optimization results in improvements for all sequences due to a more effective rate distribution across frames. As shown in Fig 7, the rate is more concentrated on the frequently used frames, such as frames 0, 4, and 8. With joint optimization, the rate of the least used frames is reduced and redistributed to frames 0, 4, and 8. This is particularly evident in the *Four People* sequence (see Figure 7). Rather than a joint optimization, one could consider establishing a rate constraint

TABLE III: Ablation study. BD-rates against HM on HEVC test sequences. Distortion is computed in the YUV420 domain.

| Motion pre-training | Joint optimization | Random Access BD-rate [%] | | | |
|---------------------|--------------------|---------------------------|-------------|-------------|------------|
| | | Class B | Class C | Class E | Average |
| | ✓ | 48.1 | 39.8 | 17.6 | 35.2 |
| ✓ | ✓ | 45.7 | 61.3 | 53.8 | 53.6 |
| ✓ | ✓ | 4.6 | 12.4 | 10.8 | 9.3 |



(a) *Four People* (HEVC E) (b) *Ritual Dance* (HEVC B)

Fig. 7: Rate distribution across frames.

for each frame type, assigning a higher constraint to less frequently used frames. However, the significant variability in rate distributions depending on sequences complicates this approach. Joint optimization addresses the issue of optimal rate distribution across frames while remaining adaptable to various sequence types.

V. LIMITATIONS

Encoding a 1920x1080 frame lasts approximately 20 minutes on an Nvidia H100 GPU. While this encoding time is comparable to other low-decoding complexity neural codecs like Cool-chic video [14] and C3 [11], it is significantly longer than that of autoencoder-based methods, such as DCVC-FM [4], which require only a single inference for encoding. However, recent studies indicate that the training time for overfitted codecs can be notably reduced by trading compression performance for shorter training [10].

In this paper, the rate of neural network parameters is not considered during the training process. The minimization loss (see eq. 4) only focuses on the latent variable rate and does not minimize the neural network parameters rate. Recent work proposes methods to put the neural network rate in the training loss function, leading to significant performance gains [23].

VI. CONCLUSION

This paper enhances overfitted codecs by improving their encoding, focusing on motion information learning and rate allocation across frames. Key contributions include a pre-trained motion module that boosts optical flow quality and a joint rate-distortion optimization. Experimental results show that the proposed codec outperforms existing overfitted codecs and competes with HEVC in the YUV420 color space while maintaining a low decoding complexity of 1300 MAC/pixel.

REFERENCES

- [1] T. Wiegand, G. Sullivan, G. Bjontegaard, and A. Luthra, "Overview of the H.264/AVC video coding standard," *IEEE Transactions on Circuits and Systems for Video Technology*, 2003.
- [2] G. J. Sullivan, J.-R. Ohm, W.-J. Han, and T. Wiegand, "Overview of the high efficiency video coding (hevc) standard," *IEEE Transactions on Circuits and Systems for Video Technology*, vol. 22, no. 12, pp. 1649–1668, 2012.
- [3] B. Bross, Y.-K. Wang, Y. Ye, S. Liu, J. Chen, G. J. Sullivan, and J.-R. Ohm, "Overview of the versatile video coding (vvc) standard and its applications," *IEEE Transactions on Circuits and Systems for Video Technology*, vol. 31, no. 10, pp. 3736–3764, 2021.
- [4] J. Li, B. Li, and Y. Lu, "Neural video compression with feature modulation," in *Proceedings of the IEEE/CVF Conference on Computer Vision and Pattern Recognition (CVPR)*, June 2024, pp. 26 099–26 108.
- [5] —, "Neural video compression with diverse contexts," in *IEEE/CVF Conference on Computer Vision and Pattern Recognition, CVPR 2023, Vancouver, BC, Canada, June 17-24, 2023*. IEEE, 2023, pp. 22 616–22 626. [Online]. Available: <https://doi.org/10.1109/CVPR52729.2023.02166>
- [6] X. Sheng, J. Li, B. Li, L. Li, D. Liu, and Y. Lu, "Temporal context mining for learned video compression," *IEEE Transactions on Multimedia*, vol. 25, pp. 7311–7322, 2023.
- [7] T. Ladune and P. Philippe, "Aivc: Artificial intelligence based video codec," in *2022 IEEE International Conference on Image Processing (ICIP)*, 2022, pp. 316–320.
- [8] T. Ladune, P. Philippe, F. Henry, G. Clare, and T. Leguay, "Cool-chic: Coordinate-based low complexity hierarchical image codec," in *Proceedings of the IEEE/CVF International Conference on Computer Vision (ICCV)*, October 2023, pp. 13 515–13 522.
- [9] T. Leguay, T. Ladune, P. Philippe, G. Clare, F. Henry, and O. Déforges, "Low-complexity overfitted neural image codec," in *2023 IEEE 25th International Workshop on Multimedia Signal Processing (MMSP)*, 2023, pp. 1–6.
- [10] T. Blard, T. Ladune, P. Philippe, G. Clare, X. Jiang, and O. Déforges, "Overfitted image coding at reduced complexity," 2024. [Online]. Available: <https://arxiv.org/abs/2403.11651>
- [11] H. Kim, M. Bauer, L. Theis, J. R. Schwarz, and E. Dupont, "C3: High-performance and low-complexity neural compression from a single image or video," in *Proceedings of the IEEE/CVF Conference on Computer Vision and Pattern Recognition (CVPR)*, June 2024, pp. 9347–9358.
- [12] H. Chen, B. He, H. Wang, Y. Ren, S.-N. Lim, and A. Shrivastava, "Nerv: neural representations for videos," in *Proceedings of the 35th International Conference on Neural Information Processing Systems*, ser. NIPS '21. Red Hook, NY, USA: Curran Associates Inc., 2024.
- [13] H. M. Kwan, G. Gao, F. Zhang, A. Gower, and D. Bull, "Hinerv: video compression with hierarchical encoding-based neural representation," in *Proceedings of the 37th International Conference on Neural Information Processing Systems*, ser. NIPS '23. Red Hook, NY, USA: Curran Associates Inc., 2024.
- [14] T. Leguay, T. Ladune, P. Philippe, and O. Déforges, "Cool-chic video: Learned video coding with 800 parameters," pp. 23–32, 2024.
- [15] M. Zhai, X. Xiang, N. Lv, and X. Kong, "Optical flow and scene flow estimation: A survey," *Pattern Recognit.*, vol. 114, p. 107861, 2021. [Online]. Available: <https://doi.org/10.1016/j.patcog.2021.107861>
- [16] Z. Teed and J. Deng, "Raft: Recurrent all-pairs field transforms for optical flow," in *Computer Vision – ECCV 2020: 16th European Conference, Glasgow, UK, August 23–28, 2020, Proceedings, Part II*. Berlin, Heidelberg: Springer-Verlag, 2020, p. 402–419. [Online]. Available: https://doi.org/10.1007/978-3-030-58536-5_24
- [17] H. Xu, J. Zhang, J. Cai, H. Rezatofghi, F. Yu, D. Tao, and A. Geiger, "Unifying flow, stereo and depth estimation," *IEEE Transactions on Pattern Analysis and Machine Intelligence*, vol. 45, no. 11, pp. 13 941–13 958, 2023.
- [18] X. Shi, Z. Huang, D. Li, M. Zhang, K. C. Cheung, S. See, H. Qin, J. Dai, and H. Li, "Flowformer++: Masked cost volume autoencoding for pretraining optical flow estimation," in *Proceedings of the IEEE/CVF Conference on Computer Vision and Pattern Recognition (CVPR)*, June 2023, pp. 1599–1610.
- [19] J. C. Lee, D. Rho, J. H. Ko, and E. Park, "Ffnerv: Flow-guided frame-wise neural representations for videos," in *Proceedings of the 31st ACM International Conference on Multimedia*, ser. MM '23. New York, NY, USA: Association for Computing Machinery, 2023, p. 7859–7870. [Online]. Available: <https://doi.org/10.1145/3581783.3612444>
- [20] F. Bossen, "Common test conditions and software reference configurations," 2013.
- [21] A. Mercat, M. Viitanen, and J. Vanne, "Uvg dataset: 50/120fps 4k sequences for video codec analysis and development," in *Proceedings of the 11th ACM Multimedia Systems Conference*, ser. MMSys '20. New York, NY, USA: Association for Computing Machinery, 2020, p. 297–302. [Online]. Available: <https://doi.org/10.1145/3339825.3394937>
- [22] Bjøntegaard, "Calculation of average psnr differences between rd-curves," April 2001.
- [23] H. M. Kwan, G. Gao, F. Zhang, A. Gower, and D. Bull, "Nvrc: Neural video representation compression," 2024. [Online]. Available: <https://arxiv.org/abs/2409.07414>